

**MINISTRY OF EDUCATION
AND TRAINING**

**VIETNAM ACADEMY OF
SCIENCE AND TECHNOLOGY**

GRADUATE UNIVERSITY OF SCIENCE AND TECHNOLOGY



NGUYỄN THANH DUNG

**PLASMA BUBBLES AND CHARACTERISTICS OF THE
EQUATORIAL IONIZATION ANOMALY OVER
VIETNAM AND ADJACENT REGION**

**SUMMARY OF GEOPHYSICS DOCTORAL THESIS
ON GEOPHYSICS**

Code: 9 44 01 11

Hanoi- 2023

The dissertation is completed at: Graduate University of Science and Technology, Vietnam Academy Science and Technology

Supervisors:

1. Supervisor 1: Dr. Le Huy Minh, Institute of Geophysics
2. Supervisor 2: Dr. Pham Thi Thu Hong, Institute of Geophysics

Referee 1: Ass. Prof. Dr. Ngo Duc Thanh

Referee 2: Ass. Prof. Dr. La The Vinh

Referee 3: Ass. Prof. Dr. Phan Thiên Hương

The dissertation will be examined by Examination Board of Graduate University of Science and Technology, Vietnam Academy of Science and Technology at

The dissertation can be found at:

1. Graduate University of Science and Technology Library
2. National Library

INTRODUCTION

Today, the Global Positioning System (GPS) is a powerful tool, useful in the ionosphere research. The ionosphere environment significantly affects the transmission of electromagnetic signals emitted by GPS satellites to ground-based receivers. The equatorial and low-latitude ionosphere has two prominent features: equatorial ionization anomaly (EIA) and plasma bubble. The EIA is characterized by a density trough around the magnetic equator and two electron density crests at about $\pm 15^\circ$ - 20° magnetic latitude (Namba & Maeda, 1939; Appleton, 1946). In fact, in the low-latitude region, the ionospheric irregularities are often associated with plasma bubbles and the medium-scale traveling ionospheric disturbance (MSTID) and spread F. Because MSTIDs occur rarely, usually only in magnetic storms, the general term nighttime ionospheric irregularity for the two phenomena of plasma bubble and MSTID has been used. The existence of ionospheric irregularities strongly affects the propagation of radio waves in the frequency range less than a few GHz, the same frequency range used in communications and navigation of GPS systems, with high disturbances can cause signal loss, while small-scale irregularities cause pseudo-range errors (Basu & Basu, 1981; Pi et al., 1997; Moraes et al., 2018). The territory of Vietnam and the adjacent region (hereafter referred to as the Southeast Asia region) locate in the EIA region (Le Huy Minh et al., 2016a). From 2005 to now, the Institute of Geophysics has built a network of continuous GPS stations (22 stations) along with several IGS stations (08 stations) in the adjacent region, which is an advantage for studying the ionosphere in Southeast Asia region.

By the importance of studying the EIA and the nighttime ionospheric irregularity, with the favorable conditions of the continuously abundant data source and the location of the study region, I have formulated a thesis with the title: "Plasma bubbles and characteristics of equatorial ionization anomaly over Vietnam and the adjacent region" under

the direction of Dr. Le Huy Minh and Dr. Pham Thi Thu Hong.

The objective of the thesis: Making clear the time variation laws of the EIA, the occurrence characteristics of the nighttime ionospheric irregularities, and the efficiency of the ionosphere models in Vietnam and the adjacent region. The specific objectives are as follows: (1) Making clear the time variation laws of the parameters of the EIA in the Southeast Asian region, the different period oscillations, and the possible causes of them; (2) Making clear the occurrence characteristics of the nighttime ionospheric irregularities in the study area. (3) Making clear the effectiveness of the International Reference Ionosphere (IRI) model, the Global TEC model from the Center of Orbit Determination in Europe Global (CODG), and the Empirical Orthogonal Function (EOF)-based TEC model in low-latitude and equatorial regions in Vietnam.

The study contents of the thesis: (1) Learning and using the algorithm to calculate Total Electron Content (TEC) from the combination of the phase and pseudo-range measurements; (2) Establishing temporal-latitudinal TEC maps for the period 2008-2021 over the Southeast Asian region; (3) Calculating the parameters of EIA peaks such as amplitude (TEC), latitude, and occurrence time to study the time variation characteristics of EIA peaks over the Southeast Asia region such as inter-seasonal variation (15 days, 27 days), semi-annual variation, annual variation, quasi-biennial oscillation (QBO), and variation with solar activity cycle; (4) The calculation of the Rate of TEC Index (ROTI) for the period 2008-2018 to study the characteristic of nighttime ionospheric irregularities over Southeast Asia region such as occurrence rate, its relationship to solar activity, and latitudinal and time distribution; the relationship between the position of the peak of irregularities occurrence and the EIA crests. (5) Using the Empirical Orthogonal Function (EOF) to model TEC values in two areas: Phuthuy (EIA crest region) and Bac Lieu (EIA trough region). Comparing the TEC values observed by the GPS receivers (GPS TEC) with

the TEC values obtained from the International Reference Ionosphere model 2016 (IRI TEC), GIMs/CODG global TEC model (CODG TEC) and TEC analyzed by EOF method (EOF TEC).

New points of the thesis: (1) Reliable identification of the EIA and nighttime ionospheric irregularities characteristics over Southeast Asia region by using GPS data series longer than one solar cycle (2008-2021). Finding out the main periodic oscillations of the ionosphere over the Southeast Asia region through EIA crest parameters which depend complexly on solar activity and possible influence factors from the lower atmosphere: ENSO, QBO, and planetary waves; (2) Showing quantitatively the position of the ionospheric irregularity peak compared to the EIA crests. The nighttime ionospheric irregularities usually appear only in the period after sunset to before midnight, for each year the ionospheric irregularities occurrence is maximum in equinoxes, depend on solar activity; the latitude of nighttime maximum irregularity occurrence is about 4° - 5° away from the daytime EIA maximum latitude equatorward. (3) It is confirmed that the EOF model can quite well simulate the diurnal variation of TEC during quiet times and magnetic storms, seasonal variation, and variation with solar activity over the Vietnam region. Comparing TEC results from GPS with TEC from global models (IRI-2016, CODG) and from EOF model shows that EOF-based TEC model predicts time variation of TEC more accurately than global models.

The structure of the thesis: In addition to the introduction and conclusion, the thesis includes 5 chapters: Chapter 1. Overview of the ionosphere, global positioning system and low-latitude ionospheric research using GPS technology; Chapter 2. Data and research methods; Chapter 3. Equatorial ionization anomaly over the Southeast Asian region; Chapter 4. The nighttime ionospheric irregularities over the Southeast Asia region; Chapter 5. Modelling the observed TEC using empirical orthogonal functions and comparing with global TEC models.

CHAPTER 1. OVERVIEW OF THE IONOSPHERE, GLOBAL POSITIONING SYSTEM, AND LOW-LATITUDE IONOSPHERIC RESEARCH USING GPS TECHNOLOGY

1.1. Overview of the ionosphere

The ionosphere is the upper atmosphere of the Earth, formed by solar radiation and cosmic radiation, located at an altitude of about 50 km to 1500 km above the ground, where ionization occurs strong enough to affect radio transmission (Breit and Tuve, 1926). The degree of ionization in the ionosphere depends on three basic factors: ionizing solar radiation energy, energy absorption coefficient of the gas components, and atmosphere density.

Based on the maximum electron density profile at a certain height, the ionosphere is divided into many layers in order of increasing altitude called layer D, layer E, layer F; in the daytime F layer is divided into F_1 and F_2 layers. The main neutral gas components in the thermosphere are O, N_2 , and O_2 . Thus, the ions produced by photoionization are O^+ , N_2^+ , O_2^+ . The equatorial and low-latitude ionosphere exist two important phenomena: EIA and nighttime ionospheric irregularity.

1.2. Overview of the global positioning system GPS

Global Positioning System (GPS) was developed by the United States government initially for military purposes. From the 1980s the United States government allowed use for civilian purposes. Therefore, the applications of GPS in many different fields have been widely researched and developed in most countries (Hofmann et al, 2001; Schaer, 1999; Đặng Nam Chinh và nnk, 2012). The GPS navigation system consists of three main parts: the space part, the control part, and the user part.

Each GPS satellite is a high-quality oscillator, it is a collection of Cesium and Rubidium atomic clocks, which is used to emit successively the two coherent carrier L1 and L2. The principal observable quantities in GPS technology are pseudo-distance and carrier phase observations.

The ionosphere is the source of the most significant errors in

positioning using satellite systems.

1.3. Overview of the situation of the ionospheric research over low-latitude regions using GPS technology

In the world, the use of GPS technology in ionosphere research began to develop strongly in the 1990s. The characteristics of diurnal, seasonal, and solar activity variation of EIA have been studied in different regions and territories such as Taiwan (Huang & Cheng, 1996; Wu et al., 2008); India (Rastogi & Klobuchar, 1990); Asia (Tsai et al., 2001); Western Pacific (Lin et al., 2001).

Ionospheric irregularities have been extensively studied over the past 70 years worldwide to understand their distribution and variability and to mitigate their bad effects on communication and positioning. In low-latitude and equatorial regions, ionosphere irregularities often associate with phenomena such as plasma bubbles, MSTIDs, sporadic E, and Spread F. Many studies were in the world on the ionosphere irregularities related to plasma bubbles as Booker, 1956; Aarons, 1997; Basu & Basu, 1981; Rama Rao et al., 2006; Li et al., 2007; Abadi et al., 2014. Some research works on MSTID as Taori et al., 2015; Hisao et al., 2018.

In Vietnam, since 2005, the application of GPS technology to study the ionosphere started with the installation of three GPS receivers in Hanoi, Hue, and Ho Chi Minh City. Some papers have studied time TEC variation using the pseudo-range measurement to calculate TEC (Le Huy Minh et al., 2006, 2014, 2016a; Tran Thi Lan et al., 2009, 2011, 2012). Le Huy Minh et al. (2016b) used the method of calculating TEC from a combination of phase and pseudo-range measurements for the magnetic storm of March 2015. Some papers have studied ionosphere scintillation (Tran Thi Lan et al., 2013, 2017).

The problem of studying equatorial ionization anomalies and nighttime plasma bubbles in low-latitude and equator regions is a research topic of interest to many scientists around the world. However, previous

studies in Vietnam have some limitations: (1) The most publications used the method of calculating TEC from pseudo-range measurement, which is less accurate than the method of combining phase and pseudo-range measurements; (2) The studies of the ionospheric scintillation (irregularity) by the S4 index only obtain by GSV4004 receivers; 3) The period oscillation characteristics of EIA crests have not been studied; 4) The distribution of ionosphere irregularities has not yet been determined quantitatively; 5) The TEC values in Vietnam have not been modeled for the prediction purpose.

In the thesis, the above limitations will be overcome with a longer data series (more than one solar cycle); the data from all GPS receivers will be used for studying nighttime ionosphere irregularity. The EIA is studied in more detail with the discovery of the main cyclic oscillations and its relationship to possible influencing factors. The distribution of nighttime ionosphere irregularities is quantitatively shown. In addition, the TEC values over the Vietnam region is initially modeled by the EOF method.

CHAPTER 2. DATA AND RESEARCH METHODS

2.1. Data using

The data used in the thesis was collected from continuous GPS stations in Vietnam and adjacent region. The geographic coordinates and magnetic latitude (epoch 2010.0) of GPS stations are listed in Table 2. Data from some international GNSS service stations are also used such as CMUM, CUSV, and CPNM in Thailand, ANMG in Malaysia, NTUS in Singapore, BAKO and JOG2 in Indonesia, and XMIS in Australia.

In addition, the thesis uses international data set as Yuma almanac data provides satellite information, F10.7 solar flux, Dst geomagnetic activity index, multivariate ENSO index MEI.v2, tropical stratospheric winds at 50 hPa (~20 km). Thesis also uses TEC data from the global ionospheric models IRI (International Reference Ionosphere-IRI) and the global TEC model GIMs/CODG.

| No | Station | Geographical Coordinate | | Magnetic latitude (2010) | Instrument | Observation time | Calculated quantity |
|----|---------|-------------------------|-----------|--------------------------|-------------|------------------|---------------------|
| | | Longitude | Latitude | | | | |
| 1 | MTEV | 102,80719 | 22,38719 | 15,92 | NETRS | 12/2009-12/2018 | TEC, ROTI |
| 2 | MLAY | 103,15385 | 22,04187 | 15,54 | NETRS | 01/2012-12/2018 | TEC, ROTI |
| 3 | LSON | 106,74906 | 21,85260 | 15,78 | CORS5700 | 12/2017-12/2021 | TEC |
| 4 | CLAN | 106,44731 | 21,67466 | 15,59 | CORS5700 | 01/2018-12/2021 | TEC |
| 5 | HUUL | 106,28931 | 21,55973 | 15,47 | CORS5700 | 12/2017-12/2021 | TEC |
| 6 | TANY | 106,07433 | 21,40704 | 15,30 | CORS5700 | 12/2017-12/2021 | TEC |
| 7 | SOCS | 105,91935 | 21,29166 | 15,17 | CORS5700 | 12/2017-12/2021 | TEC |
| 8 | DANH | 105,78528 | 21,16494 | 15,03 | CORS5700 | 12/2017-12/2021 | TEC |
| 9 | QOAI | 105,49226 | 20,95633 | 14,81 | CORS5700 | 12/2017-12/2021 | TEC |
| 10 | HOAB | 105,32750 | 20,84219 | 14,68 | CORS5700 | 12/2017-12/2021 | TEC |
| 11 | TLAC | 105,18232 | 20,69587 | 14,53 | CORS5700 | 01/2018-12/2021 | TEC |
| 12 | QHOA | 104,99143 | 20,52457 | 14,33 | CORS5700 | 12/2017-12/2021 | TEC |
| 13 | DBIV | 103,01829 | 21,38992 | 14,84 | NETRS | 11/2009- 12/2018 | TEC, ROTI |
| 14 | TGIV | 103,41803 | 21,59225 | 15,06 | NETRS | 11/2009- 12/2018 | TEC, ROTI |
| 15 | SMAV | 103,74971 | 21,05629 | 14,49 | NETRS | 6/2010- 7/2018 | TEC, ROTI |
| 16 | PHUT | 105,95872 | 21,02938 | 14,49 | GSV4004 | 2/2009- 12/2021 | TEC, ROTI |
| 17 | VINH | 105,69659 | 18,64999 | 11,91 | CORS5700 | 9/2011- 12/2021 | TEC, ROTI |
| 18 | HUES | 107,59265 | 16,45919 | 9,58 | GSV4004 | 1/2006- 10/2011 | TEC, ROTI |
| 19 | DLAT | 108,48175 | 11,94527 | 5,07 | GSV4004 | 11/2014- 12/2021 | TEC |
| 20 | HOCM | 106,55979 | 10,84857 | 3,47 | GSV4004 | 01/2008- 10/2012 | TEC, ROTI |
| 21 | HCMC | 106,80139 | 10,87808 | 3,52 | NET R9 | 2/2018- 12/2021 | TEC |
| 22 | BACL | 105,75167 | 9,26806 | 2,73 | GSV4004 | 05/2015- 12/2021 | TEC |
| 23 | CPNM | 99,37438 | 10,72465 | 2,80 | IGS station | 10/2015-04/2018 | TEC, ROTI |
| 24 | CMUV | 98,93238 | 18,76088 | 12,32 | IGS station | 01/2014-12/2021 | TEC, ROTI |
| 25 | CUSV | 100,53392 | 13,73591 | 6,43 | IGS station | 5/2008-12/ 2021 | TEC, ROTI |
| 26 | ANMG | 101,50660 | 2,78465 | -5,14 | IGS station | 02/2014-12/2021 | TEC, ROTI |
| 27 | NTUS | 103,67996 | 1,34580 | -7,05 | IGS station | 1/2008-12/ 2021 | TEC, ROTI |
| 28 | BAKO | 106,84891 | -6,49106 | -15,52 | IGS station | 1/2008- 12/2021 | TEC, ROTI |
| 29 | JOG2 | 110,37272 | -7,76377 | -16,75 | IGS station | 10/2013- 12/2021 | TEC, ROTI |
| 30 | XMIS | 105,68350 | -10,44996 | -19,99 | IGS station | 01/2008-12/2021 | TEC, ROTI |

These 30 stations (around the 105°E meridian and in the magnetic latitude range from -19.99° to 15.95°) are enough for studying EIA and nighttime ionospheric irregularities in the thesis.

2.2. Research methods

The research methods use in the thesis include the TEC calculation method, rate of TEC index (ROTI), curve fit, and some digital signal processing methods.

TEC calculation by using a combination of phase and pseudo-range measurements according to the formula:

$$STEC = \frac{1}{40.3} \frac{f_1^2 f_2^2}{f_1^2 - f_2^2} \left[(L_{1j}^i - L_{2j}^i) - (b_{\phi}^i + b_{\phi_j}) - (\lambda_1 N_{1j}^i - \lambda_2 N_{2j}^i) \right] \quad (2.6)$$

In equation (2.6), the quantity $\left[\left(b_{\phi}^i + b_{\phi j} \right) + \left(\lambda_1 N_{1j}^i - \lambda_2 N_{2j}^i \right) \right]$ is constant which have to determine (total device bias). The quantity $STEC_{\phi} = \frac{1}{40.3} \frac{f_1^2 f_2^2}{f_1^2 - f_2^2} \left(L_{1j}^i - L_{2j}^i \right)$ is precisely determined but may encounter jumps due to the phase cycle slip. The quantity $STEC_p = \frac{1}{40.3} \frac{f_1^2 f_2^2}{f_1^2 - f_2^2} \left(p_{2j}^i - p_{1j}^i \right)$ is precisely determined but less precise due to interference and multipath effects.

Possible jumps in $STEC_{\phi}$ are evaluated by following: At each epoch, $STEC_p$ is smoothed by a polynomial of degree 4, comparing $STEC_{\phi}$ with smoothed $STEC_p$ to calculate the jump magnitude. The jumps corrected STEC was compared with the STEC calculated from the GIMs/CODG model at each measurement time and each IPP site to determine the total device bias. Corrected STEC plus total device bias is converted to vertical TEC (VTEC) in a single-layer model (Klobuchar, 1986) with the height of ionosphere $h=400$ km (Zhao et al., 2009). The TEC oscillations are characterized by the rate of change of TEC with respect to time:

$$ROT = \frac{STEC_{\phi}(t + \delta t) - STEC_{\phi}(t)}{\delta t} \quad (2.8)$$

where $\delta t = 30$ s. The rate of TEC index, ROTI, is defined as standard deviation of ROT at 5-minute interval: $ROTI = \sqrt{\langle ROT^2 \rangle - \langle ROT \rangle^2}$ (2.9)

The symbol $\langle \rangle$ is the mean value of the ROT. ROT and ROTI are calculated in TECU/minute.

Signal processing methods are used as bandpass filter, wavelet transform, spectrum analysis by periodogram Lomb-Scargle, and empirical orthogonal function (EOF) method.

CHAPTER 3. EQUATORIAL IONIZATION ANOMALY IN SOUTHEAST ASIA REGION

3.1. Diurnal fluctuations of TEC at the stations

Figure 3.1 shows the calculated vertical TEC on 31/03/2021 at some stations. The TEC values at the stations clearly reflect the diurnal variation:

TEC values have the trend to increase with time from 00:00 UT (07:00 LT), reaching the maximum value in the daytime around 06:00-08:00 UT (13:00-15:00 LT) and then decreasing and having the minimum value at nighttime around 21:00-22:00 UT (04:00-05:00 LT).

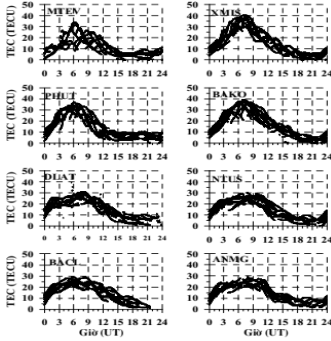


Figure 3.1. Calculated TEC on 031/2021 (31/01/2021) at some stations (from left to right, from top to bottom): MTEV, XMIS, PHUT, BAKO, DLAT, NTUS, BACL, ANMG.

The diurnal variation amplitude of TEC at stations has a clear difference: for stations at low latitudes (PHUT, BAKO), the TEC amplitude is higher than that of stations near the equator (BACL, ANMG). We can observe this more clearly when we create the temporal-latitudinal TEC maps over the Southeast Asia region.

3.2. Equatorial ionization anomaly characteristics over Southeast Asia region

3.2.1. The temporal-latitudinal TEC maps

We established the daily temporal-latitudinal TEC maps to observe the TEC distribution picture over the Southeast Asia region and study the time variation characteristics of EIA for the 2008-2021 period. The EIA crests are characterized by three parameters: amplitude, latitude, and time of occurrence.

Figure 3.5 illustrates the temporal-latitudinal monthly average TEC maps in 2014, contour interval of 5 TECU. *Figure 3.5* clearly shows that TEC has two maximum peaks on two sides of the magnetic equator, specifically in the north of the magnetic equator, the maximum is about 17-23°N, and in the south of the magnetic equator is about 5-7°S. This observed feature of TEC is known as the ionosphere's equatorial ionization

anomaly (Namba & Maeda, 1939; Appleton, 1946). These results are consistent with those of Rama Rao et al. (2006) on EIA peaks over the Indian region, and of Le Huy Minh et al. (2014) for the Southeast Asia region during the period 2006-2011.

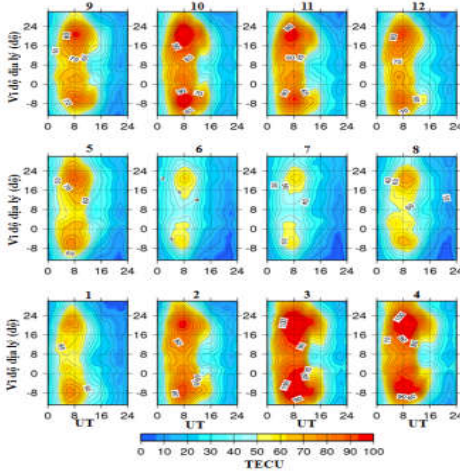


Figure 3.5. The temporal-latitude monthly average TEC maps in 2014.

3.2.2. Seasonal variation and variation with solar activity

The TEC amplitudes of the two EIA crests reach the maximum in equinoctial months (March, April, September, October), and minimum in the summer/winter months (May, June, July, August) in the northern crest/the southern crest. This observed feature is known as the EIA seasonal anomaly. The TEC amplitude at two EIA crests depends on solar activity very clearly, the TEC amplitude gradually decreases when the solar activity decreases and vice versa. The variation trend of TEC values at the two EIA peaks is consistent with the 11-year solar activity cycle, the correlation coefficient between the TEC amplitude of both EIA peaks and the F10.7 solar flux is ~ 0.90 . My correlation results are also consistent with the results published by Le Huy Minh et al., 2016a. The correlation between the TEC amplitudes at the EIA peaks with F10.7 solar flux seems to be slightly better than the correlation between the critical frequency of the F2 layer at Phu Thuy (Vietnam) - near the EIA northern crest, with sunspot number is 0.84 (Pham Thi Thu et al., 2011).

Regarding the occurrence time of two EIA crests during the period 2008-2021, both EIA peaks have the trend to appear earlier in winter than in other seasons of the year.

The location of the EIA crests has a trend to move equatorward in the winter and move poleward in the summer and equinoxes; this trend is more obviously at the southern crest than at the northern crest.

The research results on the seasonal variation of the latitude and occurrence time parameters of EIA crests in the thesis are consistent with previous studies (Tsai et al., 2001; Zhao et al., 2009; Le Huy Minh et al., 2016a).

3.2.2. Annual variation of EIA crests

During the weak solar activity periods the EIA peaks tend to move the equatorward, during the strong solar activity periods they tend to move the poleward. The annual variation of amplitudes at the two EIA crests clearly depend closely on the solar activity cycle. The TEC amplitude is high during the high solar activity period (2010-2016) and small during the weak solar activity period (2008-2009, 2018-2019). Considering the occurrence time of the EIA crests, in most years, the southern crest tends to occur later than the northern crest; in the minimum solar activity periods (2008, 2009, 2019, 2020), two peaks tend to appear at the same time.

3.3. Main periodic oscillations of EIA crests over the Southeast Asia region

In this part, I use daily time series of two peak parameters: amplitude, time of occurrence, and latitude during 2008-2021 as shown in *Figure 3.14*.

The spectral analysis results using the Lomb-Scargle periodogram method in the EIA peak parameters show the major cyclic oscillations: ~15 days, 27 days, 6 months, 1 year, quasi-biennial, 11 years and harmonics.

The results of spectral analysis using the Lomb-Scargle periodogram method for the F10.7 solar flux parameter clearly show the cyclic

oscillations: 27 days, ~ 29.5 months, 3.8 years, and 11 years (*figure 3.15*). In addition, during the range of 150-500 days periods, the spectrum of F10.7 is quite complicated, besides spectral lines of the 6-month and 1-year periods, there are many other spectral lines with larger or smaller amplitudes. Meanwhile, the spectral amplitudes of 6-month and 1-year periods in the EIA peak parameters are very clear (*figure 3.16*). Therefore, it can be said that the fluctuations of the EIA crest parameters at the 6-month and 1-year periods can be influenced by factors other than solar activity.

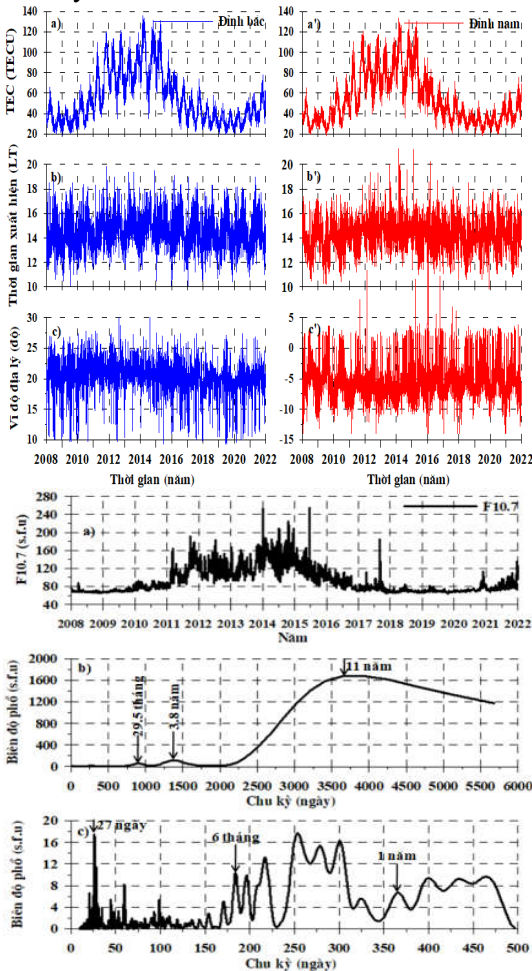


Figure 3.14. Daily variation of the two-peak parameters in the period 2008-2021: a, a') The amplitude of the north and south crests; b, b') The occurrence time of the north and south crests; c, c') The latitude of the north and south crests.

Figure 3.15. a) Daily average F10.7 solar flux during the period 2008-2021, b) Lomb-Scargle periodogram for F10.7. c) Zoom at the period range of less than 500 days.

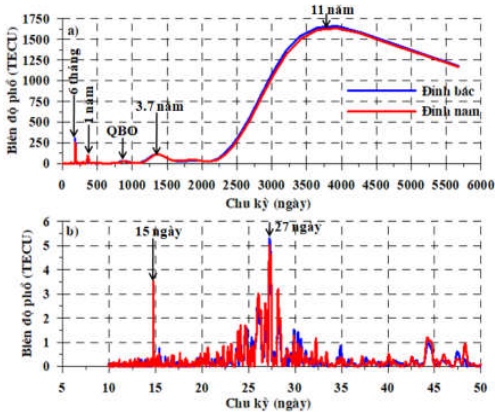


Figure 3.16. a) Lomb-Scargle periodogram for TEC amplitudes of EIA peaks for the period 2008-2021, b) exaggerated over a period range of fewer than 500 days.

3.3.1. The ~15-day period oscillation

The ~15-day period oscillation is present in all three parameters: amplitude, latitude and occurrence time of two peaks (*figure 3.21*).

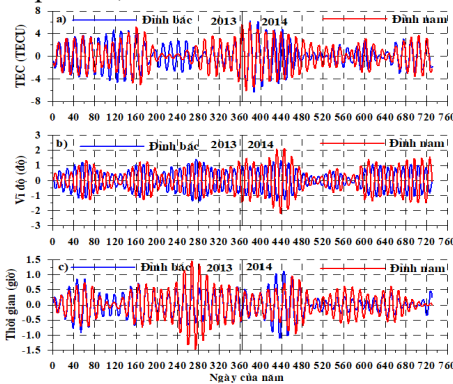


Figure 3.21. The 15-day period oscillation in parameters of two crests during the period 2013-2014: a) amplitude, b) latitude, c) time of occurrence.

This periodic oscillation is associated with the effect of planetary waves. The amplitude and occurrence time of crests are in-phase and their correlation coefficient are 0.78 and 0.74, correspondingly, meanwhile the latitudes of the two crests are out-of-phase, and the correlation coefficient between them is -0.82.

3.3.2. The 27-day period oscillation

The 27-day cycle oscillation is present in the F10.7 solar flux and EIA peak amplitude parameters. The 27-day cycle oscillation of the EIA crests is attributed to the 27 rotation of the Sun. The 27-day period oscillation of the ionosphere has a positive correlation with the 27-day

period of solar rotation. In this period, the correlation coefficient between F10.7 and the northern crest and southern crest amplitudes is 0.73 and 0.69, respectively, and between the amplitudes of the two crests is 0.95.

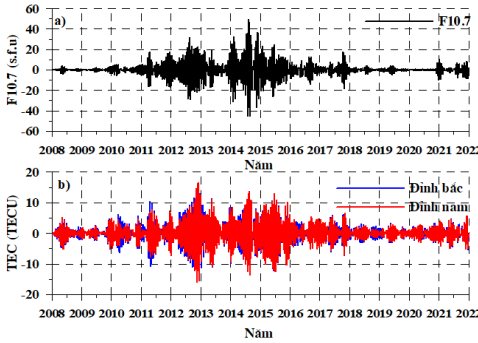


Figure 3.22. ~27 day period oscillation during the 2008-2021 period: a) F10.7, b) amplitude of EIA peaks.

3.3.3. The semi-annual oscillation

The semi-annual oscillation is present in all three parameters: amplitude, latitude, and occurrence time of two EIA crests. This oscillation of the parameters can be influenced by factors other than solar activity. The semi-annual oscillation in crest amplitude is more or less dependent on the solar activity, there is an irregularity on the 2013-2014 period. The phase relationship of the parameters between the two EIA peaks is as follows: amplitude and occurrence time of two crests have an almost in-phase relationship, but the latitude of two crests have an out-of-phase relationship. Correlation coefficients of semi-annual oscillations in the parameters of the Northern and Southern crests are: 0.99 for the TEC amplitudes, -0.77 for the latitudes and 0.75 for the occurrence times.

To investigate the possible influence of other factors on 6-month period oscillation, *Figure 3.25* presented the time variation of the MEI.v2 (Multivariate ENSO Index version 2), blue bars indicate the cold phase ENSO ($MEI.v2 \leq -0.5$) or La Niña, red bars indicate the warm phase ENSO ($MEI.v2 \geq 0.5$) or El Niño, black bars indicate neutral phase ($-0.5 < MEI.v2 < 0.5$). MEI.v2 is the combined time series of five variables as: sea level pressure, sea surface temperature, zonal and meridional components of the surface wind, and outgoing longwave radiation over tropical Pacific basin

(30°S- 30°N and 100°E- 70°W). *Figure 3.25* shows that the 6-month period oscillation amplitude at latitude of two EIA crests more or less depends on ENSO activity; in El Niño period the amplitude of semi-annual oscillation in EIA latitudes is significantly reduced compared to other periods.

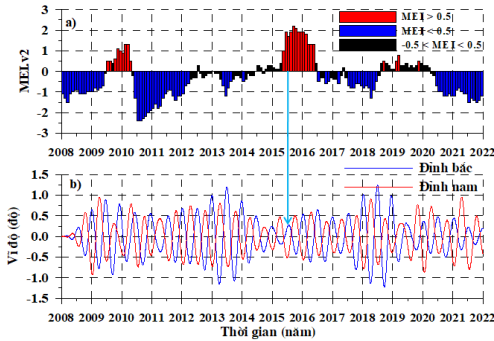


Figure 3.25. a) Multivariate ENSO index and b) 6- month period oscillation in latitude parameter of EIA crests the period of 2008-2021.

3.3.4. Annual oscillation

The annual oscillation is present in all three parameters: amplitude, latitude, and occurrence time of two EIA peaks. It is same as the semi-annual oscillation, the annual oscillation in the EIA amplitude parameters exhibits a dependence on solar activity with the irregularity on 2014, but the annual oscillation in the latitude and occurrence time parameters seems to be independent of solar activity. In this period, the amplitude and latitude of two crests are in-phase with the correlation coefficients 0.96 and 0.68 correspondingly; the occurrence times of two crests are out-of-phase with the correlation coefficient -0.77. *Figure 3.27* presented the MEI.v2 index and the annual oscillation of the latitudes of EIA crests, showing that the annual oscillation in the crests latitudes depends significantly on MEI.v2. During the El Niño periods, the annual oscillations amplitude of the crests latitudes decreases markedly, in the La Niña period, the amplitude of oscillations increases markedly. During 2015-2016, El Niño activity occurred strongly, and the amplitude of the oscillations decreased more than in other periods. So, we can confirm that the ENSO activity affects the annual oscillation in the latitude of the two EIA crests, especially for the Southern crest.

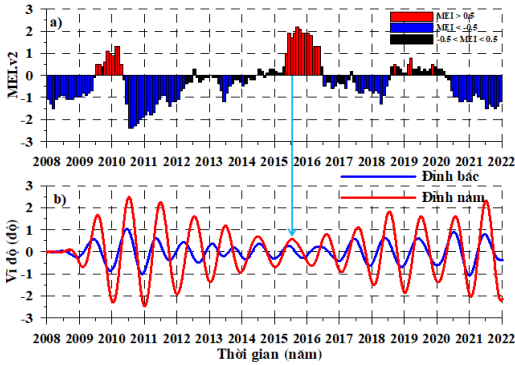


Figure 3.27. a) Multivariate ENSO index and b) the annual oscillation amplitude of crests latitude for the period 2008-2021.

3.3.5. Quasi-biennial oscillation

QBO is present in the TEC amplitude parameter at the EIA peaks with a period ranging from 18-34 months (Dung Nguyen Thanh et al., 2022). The relationship between ionospheric and atmospheric QBOs is quite complicated (*Figure 3.31*), they are in phase in the period 2010-2013, 2018-2021 and out-of-phase in the period 2014-2017.

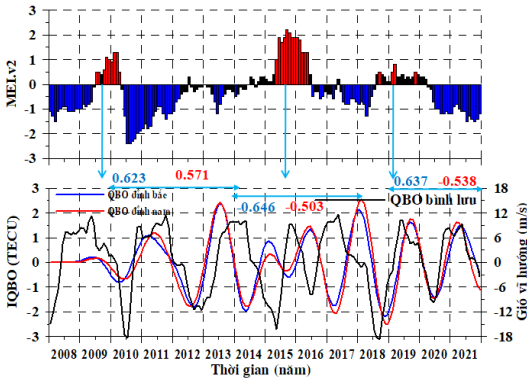


Figure 3.31. a) Multivariate ENSO index and b) QBO period oscillations of Δ TEC at two EIA crests and stratospheric QBO.

The correlation coefficients in the above periods are: 0.623, 0.637, -0.646 for the northern crest and 0.571, 0.538, -0.530 for the southern crest, respectively. In addition, a shortening of the atmospheric QBO cycle, as well as the ionospheric QBO cycle was observed in the period 2015-2016, their period is ~ 1.5 years. The above mentioned observations on the ionospheric QBO confirm that stratospheric QBO is the main factor affecting ionospheric QBO through vertical coupling between the stratosphere and the ionosphere.

CHAPTER 4. NIGHTTIME IONOSPHERIC IRREGULARITIES OVER THE SOUTHEAST ASIAN REGION

4.1. TEC variation and Rate of TEC index

Figure 4.1 is an example of TEC and ROTI diurnal variations without (a,c) and with (b, d) occurrence of nighttime ionospheric irregularity on 02/01/2015 and 15/02/2015 observed at the PHUT station. When the nighttime ionosphere irregularity occurs, the large ROTI values (*Figure 4.1d*) during from sunset to midnight.

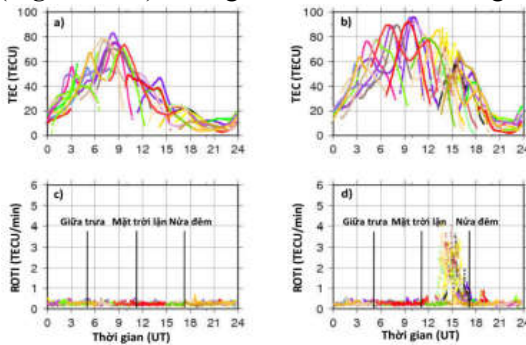


Figure 4.1. Daily variation of TEC and ROTI measured at PHUT on (a,c) 2nd January 2015 and (b,d) 15th February 2015.

4.2. Occurrence rate of ionospheric irregularities

The occurrence rates of ionospheric irregularities were maximum during equinox months (March/April and September./October) and minimum during summer (May, Jun, July and August) and winter (Jan, February, November, December). This result is consistent with previous studies that relied on different methods during high and low solar activity cycles (Fejer et al., 1999; Abdu et al., 2000; Sahai et al., 2000, Tran et al., 2017).

The ionospheric irregularities depend on solar activity. In the high solar activity periods (2012-2014), the occurrence rates of irregularities are strong. In minimum solar activity (2008, 2009 and 2018), the occurrence rates of irregularities is very small. The occurrence rate of irregularity expresses the equinoctial asymmetry. In the descending phase of solar activity (2014-2016), occurrence rates in March equinox were larger than in September equinox. In the increasing phase of solar activity (2010-2011),

the occurrence rates in September equinox were larger than in March equinox.

The correlation coefficients between the monthly occurrence rate of irregularities and F10.7 solar flux at the stations near equatorward EIA crest region were higher than at the magnetic equatorial and the poleward EIA crest regions.

4.3. The temporal-latitudinal distribution of ionospheric irregularities

The activity of irregularities are dominant in the pre-midnight sector and maximum at about 20:30-22:00 LT.

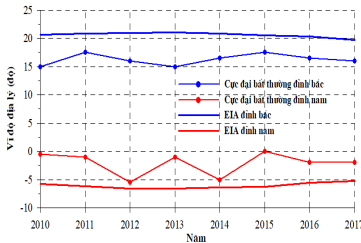


Figure 4.9. The geographic latitude of EIA crests and the geographic latitude of position where the ionospheric irregularity occurrence is maximum from 2010-2017.

We also observe the concentration of the irregularity activity at geographic latitudes about from 15°N - 18°N ($\sim 8^{\circ}\text{N}$ - 11°N magnetic latitudes) and 0° - 5°S ($\sim 7^{\circ}\text{S}$ - 12°S magnetic latitudes). The maximum irregularity occurrence location is almost in lower latitudes than the peak of EIA about 4° - 5° degrees equator-ward away from the anomaly crests (*Figure 4.9*).

CHAPTER 5. MODELLING OBSERVED TEC BY EMPIRICAL ORTHOGONAL FUNCTION AND COMPARING WITH GLOBAL TEC MODELS

5.1. Modeling TEC by EOF method

In this chapter, I will use the experimental orthogonal function analysis method mentioned in chapter 2 to initially approach the modeling of TEC values in Vietnam, especially for Phu Thuy and Bac Lieu stations. I also compare the TEC values derived from the IRI and GIMs/CODG models, TEC analyzed by the EOF method, and TEC observed from GPS receivers over Vietnam. The TEC values derived from GPS receivers, the IRI-2016 model, the CODG model, and the EOF analysis are respectively

called GPS TEC, IRI TEC, CODG TEC, and EOF TEC.

5.1.1. EOF decomposition of TEC data

Using the hourly averages of the daily TEC value (TEC(d,h): where: d is the day of observation, h is the hour of the day) observed at Phu Thuy station to perform EOF analysis. The original TEC(d,h) data are expressed as a linear combination of a small number of basis functions (Andima et al., 2019):

$$TEC(d, h) = \sum_{j=1}^n U_j(h) \times C_j(d) \quad (5.1)$$

where $C_j(d)$ is the coefficient of the base vector $U_j(h)$ with the index $j=1$ to 6. The base vector U_1 reflects the diurnal variation of TEC. The correlation coefficient between U_1 and the diurnal TEC variation is 0.981. The C_1 coefficient expressed the variation trend following to the solar activity cycle. During low solar activity period, the C_1 value is small, and vice versa, during high solar activity period, the C_1 value is high, the correlation coefficient between the coefficients C_1 and F10.7 is 0.828.

5.1.2. Analysis of EOF coefficients

TEC variation observed from GPS, TEC reconstructed from the first six EOF modes without input parameters, and TEC analyzed using EOF coefficients with input parameters are F10.7_{av} and Dst index shown in *Figure 5.5* and *5.7* for two areas Phuthuy and Baclieu, respectively. *Figures 5.5* and *5.7* show that the EOF reproduced and simulated quite well the seasonal and solar activity characteristics of TEC in Phu Thuy and Bac Lieu. The correlation coefficient between GPS TEC and EOF TEC is 0.957 for PhuThuy and 0.802 for Baclieu.

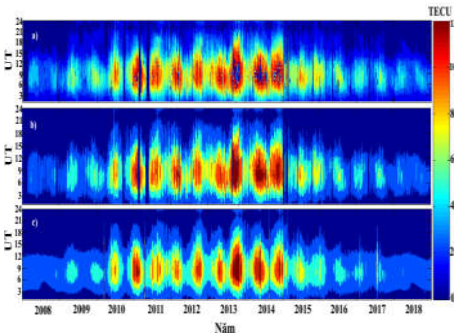


Figure 5.5. a) TEC from GPS receivers, (b) TEC reconstructed by EOF method, (c) TEC analyzed by EOF method with input F10.7_{av} and Dst index parameters at Phuthuy the period of 2008-2018.

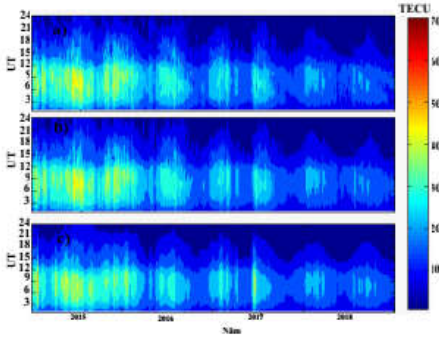


Figure 5.7. a) TEC from GPS receivers, (b) TEC reconstructed by EOF method, (c) TEC analyzed by EOF method with input $F_{10.7_{av}}$ and Dst parameters at Baclieu the period of 2015-2018.

5.2. Comparing observed TEC with TEC from models

5.2.1. For quiet days

The quiet days choice in the equinoxes (March and September) and the solstice months (June and December) are based on the magnetic activity $K_p < 3$ and the Dst indices to calculate the diurnal variation of TEC by EOF method, the results are shown in *Figure 5.9* and *Figure 5.15*.

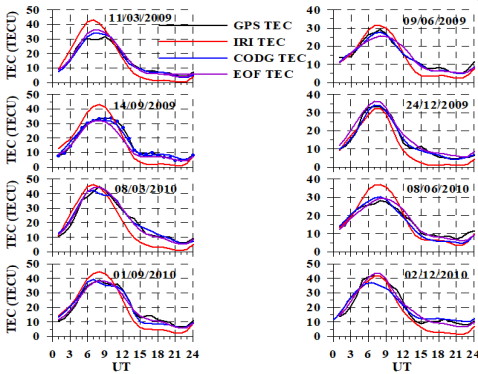


Figure 5.9. Diurnal variation of GPS TEC, IRI TEC, CODG TEC, and EOF TEC values for some quiet days during 2009-2010 at Phuthuy.

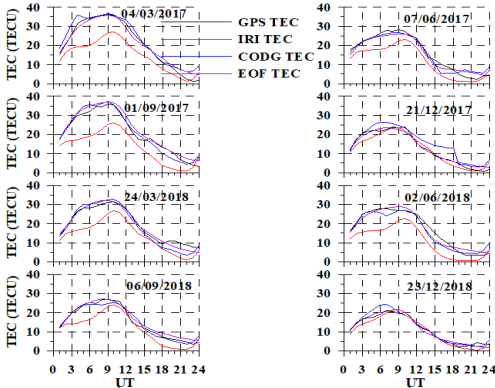


Figure 5.15. Diurnal variation of GPS TEC, IRI TEC, CODG TEC, and EOF TEC values for some quiet days during 2017-2018 at Baclieu.

Figure 5.9 shows that IRI overestimated GPS TEC values, CODG and EOF quite well estimated GPS TEC values for the Phuthuy station. Figure 5.15 shows that IRI almost underestimates GPS TEC values while CODG and EOF quite well estimate GPS TEC values for the Baclieu station.

5.2.2. For magnetic storm days

To evaluate the effectiveness of the EOF method applied to the analysis of TEC values during magnetic storms, I simulated TEC for two magnetic storms in two Phuthuy and Baclieu regions (figure 5.16 and 5.17). The EOF and CODG models reproduced the TEC values in the ionosphere better than the IRI model.

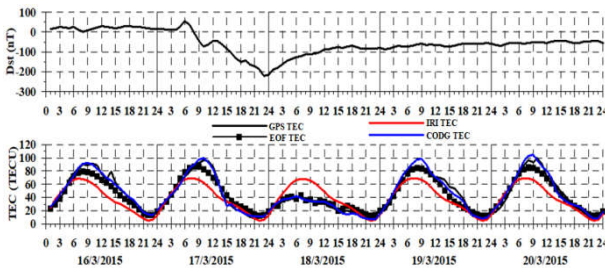


Figure 5.16. GPS TEC, EOF TEC, IRI TEC, CODG TEC during the magnetic storm on 16-20 March 2015 at Phuthuy.

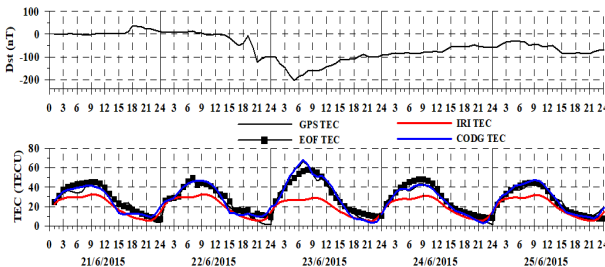


Figure 5.17. GPS TEC, EOF TEC, IRI TEC, CODG TEC during the magnetic storm on 21-25 June 2015 at Baclieu.

5.3. Error evaluation of models

The root mean square error (RMSE) parameter has been used to evaluate the difference between TEC values derived from the EOF analysis, the IRI model, and the CODG model with TEC values derived from GPS receivers at Phuthuy and Baclieu. CODG predicted the TEC at Phuthuy with the least RMSE values (except March), followed by the EOF model

(except December) in 2009. In the same year, IRI 2016 predicted TEC at Phuthuy with the RMSE almost to be the highest. In 2013, the RMSE had the highest value for IRI TEC and the lowest value for CODG TEC. Diurnal RMSE variation in 2015 was higher than in 2018 (weak solar activity) at Baclieu. At Baclieu, IRI predicts the worst TEC, EOF predicts the best TEC.

CONCLUSIONS AND RECOMMENDATIONS

CONCLUSIONS

From the results obtained in studying the characteristics of the EIA and the nighttime ionospheric irregularities over Southeast Asia region using continuous GPS data over Vietnam and adjacent region in the thesis, I have drawn some conclusions as followings:

1. The time and latitude TEC maps for the period 2008-2021 in the Southeast Asia region show a very clear two crests EIA structure, the north crest is around $17\text{-}22^{\circ}\text{N}$, and the south crest is around $5\text{-}7^{\circ}\text{S}$. The laws of diurnal, seasonal, and solar activity variation found in the thesis are consistent with previous EIA research results in the low-latitude and equatorial regions in the world (Tsai et al. ., 2001, Rama Rao et al., 2006, Zhao et al., 2009) as well as in Vietnam and the adjacent region (Le Huy Minh et al., 2014, 2016a).

2. The EIA crests have the major period oscillations:

- ~ 15 day period oscillation exists in three parameters, amplitude and occurrence time of two crests are in phase with correlation coefficients 0.78 and 0.74 respectively, crests latitude are anti-phase with a correlation coefficient of -0.82, this oscillation is thought to be related to the activity of planetary waves propagating from the lower atmosphere.

- The ~ 27 -day period oscillation occurs only in the EIA crest amplitude which is related to the ~ 27 -day rotation of the Sun. The correlation coefficient between the 27-day period fluctuations at the north (south) crest amplitude and F10.7 is 0.73 (0.69).

- The semiannual oscillation is present in all three crest parameters. The magnitude of the crests dependent more or less on solar activity with irregularity in 2013-2014, but the occurrence time and latitude seem not to be. The amplitude and time of appearance of two peaks are in phase with the correlation coefficient of 0.99 and 0.75, respectively, the latitudes of the two crests are out-of-phase with correlation coefficient of -0.77. The latitude of the two peaks depends on ENSO activity; during El Niño period in this period the oscillation amplitude of the crest latitude is significantly reduced.

- The annual oscillations are also present in all three crest parameters. The amplitudes of crests dependent more or less on solar activity with irregularity in 2014, but occurrence time and latitude seem not to be. The amplitude and latitude of two peaks are in phase, with the correlation coefficients of 0.96 and 0.68, respectively, the occurrence times of two peaks are out-of-phase with the correlation coefficient of -0.77. The latitude of the two peaks strongly depends on ENSO activity; during El Niño period in this period the oscillation amplitude of the crest latitude is significantly reduced, especially for the southern crest.

- QBO is present in the TEC amplitude of both EIA crests with periods ranging between 18 and 34 months. The atmospheric QBO is the main factor causing the ionospheric QBO.

3. In the Southeast Asia region, the rate of occurrence of ionospheric irregularities is maximum in the equinoxes and minimum in the solstices. The irregularity activity predominates around midnight and reaches the maximum at about 20:30-22:00 LT. The maximum occurrence of the nighttime ionospheric irregularities located at latitude about $4\text{-}5^\circ$ lower than the daytime EIA crests towards the equator.

4. The EOF analysis method predicted well the diurnal variation of TEC values over Phu Thuy and Bac Lieu stations. Meanwhile, the IRI model overestimated or underestimated diurnal variation of TEC values

over these two regions. The EOF model well simulates seasonal and solar activity variations. Magnetic storm effects affecting ionospheric TEC values are better reflected by EOF analysis than by IRI or CODG models.

RECOMMENDATIONS

From the results obtained in the thesis, I suggest some research issues that need to be continued as follows:

- Estimation of the QBO signature in the latitude and occurrence time of the EIA crests.

- Studying the relationship between the variation of EIA crests and the activity of the Earth's magnetic field.

- The time variation of the equatorial ionization anomaly depends on many factors as solar activity, Earth's magnetic field, and the lower atmosphere, so it is necessary to use general circulation models like TIE-GCM (Thermosphere-Ionosphere-Electrodynamics General Circulation Model) to understand the origin of the variation of the observed parameters of the equatorial ionization anomaly crests.

- Studying the characteristics of the nighttime ionospheric irregularities over the Southeast Asia region which separately related to the plasma bubbles (source from the equatorial region) and to the MSTID (source from mid-latitude region).

LIST OF THE PUBLICATIONS RELATED TO THE DISSERTATION

1. **Dung Nguyen Thanh**, Minh Le Huy, Christine Amory-Mazaudier, Rolland Fleury, Susumu Saito, Thang Nguyen Chien, Thanh Le Truong, Hong Pham Thi Thu, Thanh Nguyen Ha, Mai Nguyen Thi, Que Le, 2022. Ionospheric quasi-biennial oscillation of the TEC amplitude of the equatorial ionization anomaly crests from continuous GPS data in the Southeast Asian region, *Vietnam Journal of Earth Sciences*, <https://doi.org/10.15625/2615-9783/17490>. (Tập chí scopus).
2. **Dung Nguyen Thanh**, Minh Le Huy, Christine Amory-Mazaudier, Rolland Fleury, Susumu Saito, Thang Nguyen Chien, Hong Pham Thi Thu, Thanh Le Truong, Mai Nguyen Thi, 2021. Characterization of ionospheric irregularities over Vietnam and adjacent region for the 2008-2018 period, *Vietnam Journal of Earth Sciences*, doi:10.15625/2615-9783/16502. (Tập chí scopus).
3. Hong Pham Thi Thu, Christine Amory-Mazaudier, Minh Le Huy, Susumu Saito, Kornyanat Hozumi, **Dung Nguyen Thanh**, Ngoc Luong Thi, 2022. Nighttime morphology of vertical plasma drifts over Vietnam during different seasons and phases of sunspot cycles, *Adv. Space Res.*, **70**, 411-426, <https://doi.org/10.1016/j.asr.2022.04.010>. (Tập chí SCIE).
4. Hong Pham Thi Thu, Christine Amory-Mazaudier, Minh Le Huy, **Dung Nguyen Thanh**, Hung Luu Viet, Ngoc Luong Thi, Kornyanat Hozumi, Thanh Le Truong, 2020. Comparison between IRI-2012, IRI-2016 models and F2 peak parameters in two stations of the EIA in Vietnam during different solar activity periods, *Adv. Space Res.*, **68**, 2076-2092, <https://doi.org/10.1016/j.asr.2020.07.017> (Tập chí SCIE).